

## Site-Selective Anatomy of Step-by-Step Reactions in Ligand–Receptor Bonding Processes Using Dynamic Force Spectroscopy

Atsushi Taninaka, Osamu Takeuchi, and Hidemi Shigekawa\*

*Institute of Applied Physics, CREST-JST, University of Tsukuba, Tsukuba, Ibaraki 305-8573, Japan*

Received June 17, 2009; accepted July 2, 2009; published online July 24, 2009

We demonstrate a methodology that realizes the site-selective anatomy of molecular interactions at the single-molecule level. With the combination of cross-linkers and the atomic force microscope that we developed to enable a precise analysis by dynamic force spectroscopy, direct and bridged interactions at each reaction site in a typical ligand–receptor system, streptavidin–biotin complex, were clearly distinguished and individually analyzed for the first time, providing a greater understanding of step-by-step progress of the bonding process. The bridging molecule at the middle reaction sites, which was assumed to be the water molecule in the previous study, was identified as the phosphate molecule. © 2009 The Japan Society of Applied Physics

DOI: 10.1143/APEX.2.085002

The variety and selectivity of interactions between a pair of functional molecules, for example, DNA, ligand–receptor and antigen–antibody systems, play essential roles in biological processes and molecular devices based on molecular recognition properties. As is the case for a protein molecule, however, functions often originate from structurally complex processes. Furthermore, such interactions include complicated many-body effects arising, for example, from solvent parameters and the manifold structures of functional molecules, which prevent the design of detailed functions in predetermined structures.<sup>1,2)</sup> Therefore, probing the step-by-step bonding processes induced by the individual interactions in a molecular complex and their variation with the surrounding conditions is a key factor for enabling further advances in biophysics and chemistry and their applications.

The streptavidin–biotin complex is a typical ligand–receptor system and has been extensively studied.<sup>3–8)</sup> Since this system has a complicated structure when considering its chemical reactions, a variety of processes are expected to occur in this system depending on the operating conditions. Therefore, probing to obtain a deeper understanding of the energy landscapes of individual interaction sites of this typical system is not only important in itself, but will also provide a foundation for designing and controlling the mechanism of chemical reactions between two complicated functional molecules. Dynamic force spectroscopy (DFS) is a technique that enables us to study interaction between molecules at the single-molecule level.<sup>3–8)</sup> In a pioneering study on the DFS of the streptavidin–biotin complex, a potential landscape with two barrier widths (0.12 and 0.5 nm) was observed, which was assumed to be due to direct hydrogen bonding and an indirect interaction via bridged water molecules.<sup>3)</sup> However, the results obtained from previous experiments are not comprehensively understood, and some controversies remain in explaining the mechanism of the bond structures.<sup>8–14)</sup> In addition, basic analysis methods for DFS are still being developed.<sup>8–14)</sup> Therefore, a more detailed study is necessary to achieve further advances.

In this paper, we present a new methodology realizing the site-selective anatomy of molecular interactions based on DFS. Direct and bridging interactions at each reaction site in the streptavidin–biotin complex were clearly distinguished

and individually analyzed for the first time using an atomic force microscope (AFM) system that we have developed, providing a greater understanding of the step-by-step progress of the bonding process.

In DFS, the unbinding force applied to a molecular pair is increased at a constant rate, and the force required to rupture the bond is measured. When the DFS measurement is carried out by AFM with a cross-linker molecule, a constant retraction velocity does not result in a constant loading rate because of the stretching of the cross-linker molecule. We have developed an AFM system with a feedback loop, which enables the fine control of low loading rates to reduce the effect of the soft cross-linker that connects a sample molecule to the tip or substrate.<sup>8–10,12)</sup> In addition, the AFM system enables us to realize a high sampling rate to obtain a sufficient amount of data at a high loading rate. Furthermore, since AFM measurement is stable under various pHs, different buffer solutions with different pH values can be used.

To perform the site-selective analysis, we prepared two types of cross-linker for controlling the depth of the active reaction sites by changing the effect of the geometry of the system on the bond formation site. Namely, streptavidin was fixed to a self-assembled monolayer (SAM) of (a) 8-amino, 1-octanethiol molecules on a Au-coated substrate via a biotin–PEG–COO–NHS molecule (flexible condition) or (b) 1,10-decanedithiol/1-octanethiol (1/100 ratio) mixed solution on a Au-coated substrate via a streptavidin–maleimide structure (modified condition). For both cases, a closely packed SAM with amino groups was formed on a gold-coated cantilever and a biotin (biotin–PEG) molecule was fixed onto the probe apex. As shown in Fig. 1, the biotin molecule attached to the cantilever can enter deep into the binding pocket and conjugate even with the inner amino acid residues in streptavidin under the flexible condition (a). In contrast, under the modified condition (b), this process is prevented owing to a lack of flexibility, and bonding only at the middle and outer sites is achieved. Since the SAM formed on the substrate has a hydrophobic characteristic the modified condition may increase the effect of the hydrophobic feature of the substrate surface on the formation of hydrogen bond. In this study, this method of site-selective analysis is demonstrated to be effective.

To avoid multiple-bonding events, as mentioned above, the density of the target molecules in the SAM was reduced so that the probability of bonding became 5–10% for each tip–sample approach. Furthermore, only single ruptures were

\*E-mail address: hidemi@ims.tsukuba.ac.jp

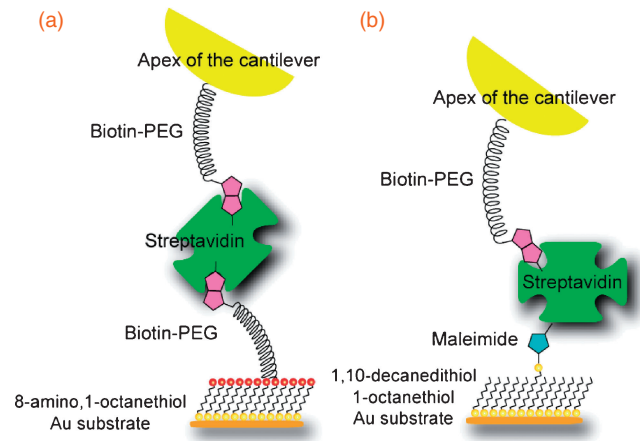


**Fig. 1.** Schematic illustration of site-selective analysis using two types of cross-linker: (a) flexible condition and (b) modified condition. The distances between streptavidin and substrate are  $\sim 30$  nm for the flexible condition and  $\sim 1.5$  nm for the modified condition, respectively.

counted to remove the errors caused by the effect of multiple-rupture events on the analysis. The loading rate was controlled between 10 and  $10^5$  pN/s, and 5000–10000 approach and retract cycles were carried out to form a histogram for each loading-rate measurement. Information concerning the energy landscape of the interaction was derived from the relationship between the modal rupture force obtained from the histogram and the loading rate of the unbinding force.

Figure 2(a) shows the relationships between the modal rupture force and the logarithm of the loading rate obtained in a 0.01 M phosphate buffered solution (PBS, pH 7.4) for the (a) flexible condition and (b) modified condition. The inset shows a typical histogram of the rupture forces obtained for the fixed condition in a pH 7.4 phosphate-buffered solution at the loading rate of  $2.95 \times 10^2$  pN/s, where the modal rupture force is 31.0 pN. For the flexible condition, the gradient of the slope exhibits a marked increase at  $2 \times 10^3$  pN/s. In accordance with the DFS theory,<sup>8)</sup> each slope corresponds to an unbinding process related to one potential barrier, and the distance of the barrier position from the potential bottom,  $x_b$ , can be deduced from the reciprocal of the gradient.<sup>3–14)</sup> The potential barrier positions were estimated from the two slopes to be  $0.13 \pm 0.01$  and  $0.63 \pm 0.09$  nm, which are consistent with the values of 0.12 and 0.5 nm obtained in a previous study.<sup>3)</sup>

In contrast, under the modified condition, only one slope was observed, and the potential barrier position estimated from this slope was  $0.68 \pm 0.05$  nm. To confirm the validity of this result, we plotted the values from 23 histograms obtained using three cantilevers with different spring constants and shapes (6 pN/nm, rectangular, Au-coated; 30 pN/nm, rectangular, Au-coated; and 20 pN/nm, triangular, noncoated  $\text{Si}_2\text{N}_3$ ). No marked dependence on the type of cantilever was observed.

As proposed in a recent study, the potential barrier position can be estimated by analysis of the shape of the rupture force distribution.<sup>8)</sup> The solid green line in the inset shows a theoretical fitting curve, and the potential barrier position  $x_b$  obtained from the distribution based on the

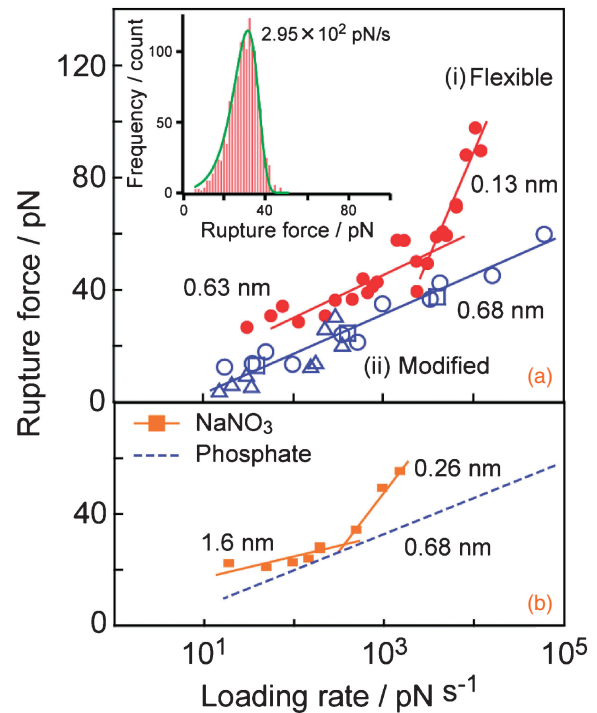


**Fig. 2.** (a) Relationship between the modal rupture force and the logarithm of the loading rate. Results are obtained for the flexible [(i) red] and modified [(ii) blue] conditions using 0.01 M phosphate (pH 7.4) solution ( $\circ$ : 6 pN/nm, rectangular, Au-coated,  $\square$ : 30 pN/nm, rectangular, Au-coated, and  $\triangle$ : 20 pN/nm, triangular, noncoated  $\text{Si}_2\text{N}_3$ ). The inset shows a typical histogram obtained for modified condition in PBS (pH 7.4) at loading rate of  $2.95 \times 10^2$  pN/s. Solid green line represents a theoretical fitting curve based on the method of analysis proposed in ref. 8. The measurement of barrier position is mainly affected by error of the spring constant of the cantilever (10–20%). (b) Similar experimental result obtained in 0.05 M sodium nitrate buffer solution (pH 7) under modified condition (orange lines). The result obtained for the 0.01 M phosphate (pH 7.4) solution shown in (a) is drawn together for comparison (blue dashed line).

method in ref. 8 is at 0.69 nm. The result is consistent with the barrier position of 0.68 nm obtained from the slope of Fig. 2(a) and validates the measurements.

From the observation that the potential barrier of 0.13 nm was obtained only under the flexible condition and the prediction by molecular dynamics (MD) calculation, in which hydrogen bonding with a rupture distance shorter than 0.2 nm is attributed to the bonds formed at an inner site,<sup>15,16)</sup> the barrier position of 0.13 nm is related to the direct bonding of inner amino acid residues such as ASP128, TYR43, and ASN23 with the biotin molecule [Fig. 3(c)].<sup>17,18)</sup> On the other hand, from the results of an MD calculation, a potential barrier with a distance greater than 0.4 nm cannot exist without a salt molecular bridge for the case of phosphate.<sup>15,16)</sup> This suggests that the bond related to the potential barrier positions of 0.68 and 0.63 nm is formed by molecular bridging between the amino acid residues at the middle reaction sites and the biotin molecule.

To analyze the origin of the potential barriers of 0.68 and 0.63 nm in more detail, we changed the buffer solution from 0.01 M phosphate (pH 7.4) to 0.05 M sodium nitrate (pH 7), and measurements were performed under the modified condition. As shown in Fig. 2(b), the slope changed at a loading rate of about  $10^2$ – $10^3$  pN/s, and the two potential

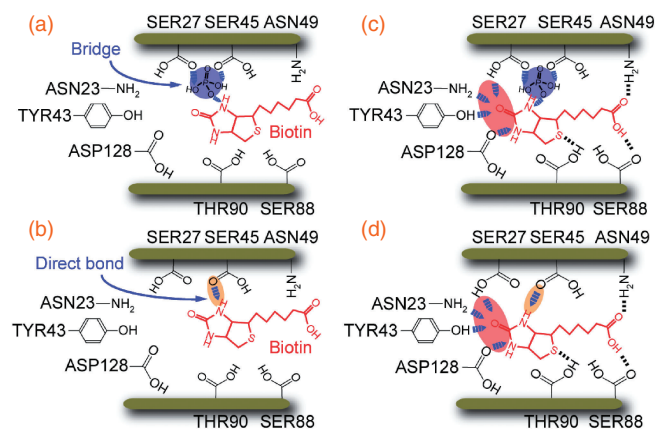


**Fig. 3.** Step-by-step progress of bonding. Bonds represented by thick blue dots are those determined in this study.

barrier positions were estimated to be  $0.26 \pm 0.03$  and  $1.6 \pm 0.75$  nm. In addition, from the results of an MD calculation,<sup>16)</sup> the direct bond between SER45 and the biotin molecule has a potential barrier position of 0.26 nm. Therefore, the bond related to the potential barrier position of  $0.26 \pm 0.03$  nm is attributed to the potential barriers formed by direct bonding between the biotin molecule and the middle reaction sites of streptavidin such as SER45. Since the bond of the potential barriers of 0.68 and 0.63 nm does not exist in the 0.05 M nitrate solutions, the bond is formed by the phosphate molecules in the buffer solution, instead of the water molecules, in contrast to the mechanism predicted in a previous study.<sup>3)</sup> In fact, no rupture events were observed in purified water.

These results indicate that formation of hydrogen bond at the inner site was inhibited under the modified condition, as expected. As a result, bonding at the inner sites or middle sites were distinguished and separately analyzed using the flexible and modified conditions. The potential barrier for the direct bond at SER45 is consistent with the theoretical prediction. Since nitrate molecules do not induce a bridge bonding, a slight change in the molecular structure of the solvent may affect the bonding interaction. The origin for the bond with a large barrier position ( $\text{NaNO}_3$ :  $1.6 \pm 0.75$  nm) is not clear. Further experiments on these issues are now in progress.

The lifetime of bonds can be estimated from the intercept obtained by extrapolating the linear relationship between the modal rupture force and the logarithm of loading rate,<sup>8)</sup> as shown in Fig. 2.<sup>3–14)</sup> The rupture forces obtained for the flexible condition were larger than those for the modified condition at all loading rates, as shown in Fig. 2, and the lifetimes obtained for the flexible and modified conditions were 6.4 and 1.0 s, respectively. From the result of the flexible condition (6.4 s), the lifetime for streptavidin–biotin–PEG is estimated to be 12.8 s.<sup>5)</sup> This value is ten times larger than that of the modified condition. This is caused by the fact that the direct bonds with the inner amino acid residues such as ASP128, TYR43, and ASN23 are stable under the flexible condition because the biotin molecule attached to the cantilever can enter deep into the binding pocket, or the effect of hydrophobic interaction from the substrate is less than that under the modified condition. From the experi-

mental results, lifetime clearly depends on the type of bond (direct or bridged) and the formation site rather than the type of buffer. At the middle sites, the lifetime of the direct bond was shorter than that of the bridged bond, which was also directly observed for the first time.

The observed results enable us to discuss the step-by-step progress of the bonding process: (1) A biotin molecule is trapped at the middle sites via the bridging of buffer molecules since the bridge is the longest bond. (2) The structure of the indirect interaction remains (in the case of phosphate solution) or direct hydrogen bonding occurs (other solutions), depending on the relative strength of the interaction [Figs. 3(a) and 3(b)]. (3) The bonding of the inner sites with the ureido oxygen of the biotin molecule occurs. (4) Bonding occurs between the outer sites and the end group of the biotin molecule (carboxyl), as illustrated in Figs. 3(c) and 3(d).

In conclusion, we demonstrated a methodology that enables the site-selective anatomy of molecular interactions at the single-molecule level. Using the combination of cross-linkers and an atomic force microscope that we developed to enable precise analysis by DFS, direct and bridging interactions at each reaction site in a ligand–receptor system were clearly distinguished and individually analyzed for the first time, providing a greater understanding of the step-by-step progress of the bonding process. This methodology will provide a foundation for further advances in biophysics and chemistry and their applications, such as designing and controlling the mechanism of chemical reactions between functional molecules.

**Acknowledgment** This work was supported in part by a Grant-in-Aid for Scientific Research from the Ministry of Education, Culture, Sports, Science, and Technology of Japan (Yong Scientists B). We thank Ms. Rie Yamashita, for her help in preparing this paper.

- 1) J. D. Badjić, V. Balzani, A. Credi, S. Silvi, and J. F. Stoddart: *Science* **303** (2004) 1845.
- 2) S. Yasuda, I. Suzuki, K. Shinohara, and H. Shigekawa: *Phys. Rev. Lett.* **96** (2006) 228303.
- 3) R. Merkel, P. Nassoy, A. Leung, K. Ritchie, and E. Evans: *Nature* **397** (1999) 50.
- 4) C. Yuan, A. Chen, R. Kolb, and V. T. Moy: *Biochemistry* **39** (2000) 10219.
- 5) A. B. Patel, S. Allen, M. C. Davies, C. J. Roberts, S. J. B. Tendler, and P. M. Williams: *J. Am. Chem. Soc.* **126** (2004) 1318.
- 6) M. O. Piramowicz, P. Czuba, M. Targosz, K. Burda, and M. Szymoński: *Acta Biochim. Pol.* **53** (2006) 93.
- 7) J. Wong, A. Chilkoti, and V. T. Moy: *Biomol. Eng.* **16** (1999) 45.
- 8) O. Takeuchi, T. Miyakoshi, A. Taninaka, K. Tanaka, D. Cho, M. Fujita, S. Yasuda, S. P. Jarvis, and H. Shigekawa: *J. Appl. Phys.* **100** (2006) 074315.
- 9) E. Evans and K. Ritchie: *Biophys. J.* **72** (1999) 1541.
- 10) E. Evans and K. Ritchie: *Biophys. J.* **76** (1999) 2439.
- 11) A. Pierres, D. Touchard, A.-M. Benoliel, and P. Bongrand: *Biophys. J.* **82** (2002) 3214.
- 12) C. Friedsam, A. K. Wehle, F. Kühner, and H. E. Gaub: *J. Phys.: Condens. Matter* **15** (2003) S1709.
- 13) F. Pincet and J. Husson: *Biophys. J.* **89** (2005) 4374.
- 14) J. Husson and F. Pincet: *Phys. Rev. E* **77** (2008) 026108.
- 15) H. Grubmüller, B. Heymann, and P. Tavan: *Science* **271** (1996) 997.
- 16) J. Zhou, L. Zhang, L. Yongsheng, H.-K. Tsao, Y.-J. Sheng, and S. Jiang: *J. Chem. Phys.* **125** (2006) 104905.
- 17) P. C. Weber, D. H. Ohlendorf, J. J. Wendoloski, and F. R. Salemme: *Science* **243** (1989) 85.
- 18) B. A. Katz: *J. Mol. Biol.* **274** (1997) 776.